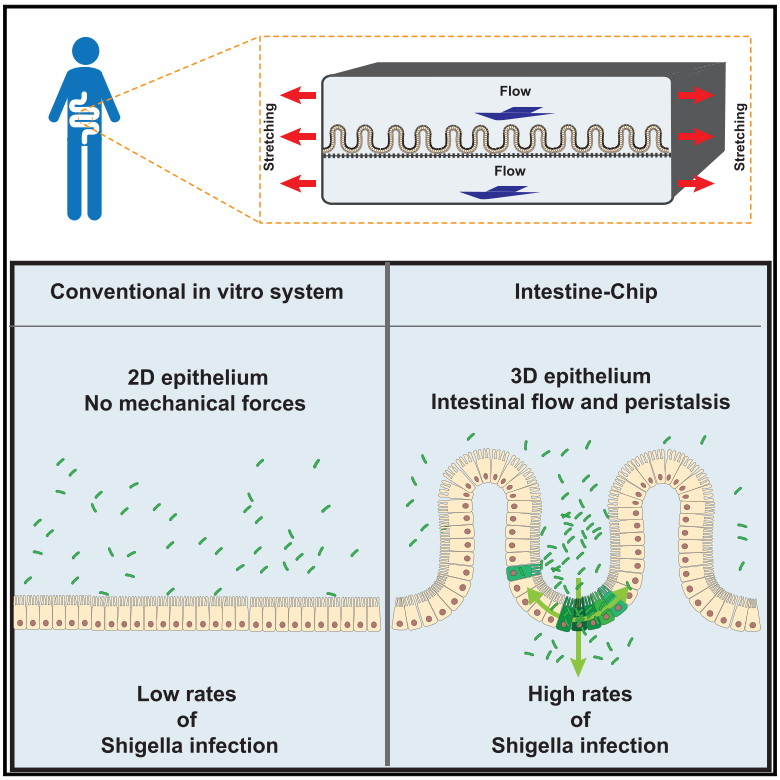
Short Article

Cell Host & Microbe

Bioengineered Human Organ-on-Chip Reveals Intestinal Microenvironment and Mechanical Forces Impacting *Shigella* Infection

Graphical Abstract



Authors

Alexandre Grassart, Valérie Malardé, Samy Gobba, ..., Benoit Marteyn, Philippe Sansonetti, Nathalie Sauvonnet

Correspondence

alexandre.grassart@pasteur.fr (A.G.), nathalie.sauvonnet@pasteur.fr (N.S.)

In Brief

Grassart et al. employ Organ-on-Chip to interrogate the impact of intestinal mechanical forces on *Shigella* infection. In the 3D microenvironment, *Shigella* infects enterocytes from the apical side, exploiting the crypt-like invaginations for early colonization, while intestinal peristalsis enhances invasion. Collectively, Organ-on-Chip reveals that *Shigella* leverages the intestinal microarchitecture and mechanical forces.

Highlights

- Intestine-Chip reveals that *Shigella* infects enterocytes efficiently from the gut lumen
- The crypt-like structure of the intestine is critical for *Shigella* adhesion
- Peristaltic motion (mechanical forces) enhances *Shigella* invasion
- *Shigella* exploits intestine architecture and mechanical forces to maximize infectivity

Grassart et al., 2019, Cell Host & Microbe *26*, 435–444
September 11, 2019 © 2019 Elsevier Inc.
https://doi.org/10.1016/j.chom.2019.08.007

CellPress

Cell Host & Microbe
Short Article

Bioengineered Human Organ-on-Chip Reveals Intestinal Microenvironment and Mechanical Forces Impacting *Shigella* Infection

Alexandre Grassart,[1,*] Valérie Malardé,[1] Samy Gobba,[2,6] Anna Sartori-Rupp,[3,6] Jordan Kerns,[4] Katia Karalis,[4] Benoit Marteyn,[1,5] Philippe Sansonetti,[1] and Nathalie Sauvonnet[1,7,*]
[1]Unité de Pathogénie Microbienne Moléculaire, Institut Pasteur, INSERM U1202, 28 rue du Docteur Roux, 75015 Paris, France
[2]Biomaterials and Microfluidics Facility, C2RT, Institut Pasteur, 28 rue du Docteur Roux, 75015 Paris, France
[3]Unité de Bio-imagerie ultra-structurale, C2RT, Institut Pasteur, 28 rue du Docteur Roux, 75015 Paris, France
[4]Emulate, Inc., 27 Drydock Avenue, Boston, MA 02210, USA
[5]IBMC, Université de Strasbourg, CNRS UPR 9002 (ARN), Strasbourg, France
[6]These authors contributed equally
[7]Lead Contact
*Correspondence: alexandre.grassart@pasteur.fr (A.G.), nathalie.sauvonnet@pasteur.fr (N.S.)
https://doi.org/10.1016/j.chom.2019.08.007

SUMMARY

Intestinal epithelial cells are constantly exposed to pathogens and mechanical forces. However, the impact of mechanical forces on infections leading to diarrheal diseases remains largely unknown. Here, we addressed whether flow and peristalsis impact the infectivity of the human pathogen *Shigella* within a 3D colonic epithelium using Intestine-Chip technology. Strikingly, infection is significantly increased and minimal bacterial loads are sufficient to invade enterocytes from the apical side and trigger loss of barrier integrity, thereby shifting the paradigm about early stage *Shigella* invasion. *Shigella* quickly colonizes epithelial crypt-like invaginations and demonstrates the essential role of the microenvironment. Furthermore, by modulating the mechanical forces of the microenvironment, we find that peristalsis impacts *Shigella* invasion. Collectively, our results reveal that *Shigella* leverages the intestinal microenvironment by taking advantage of the microarchitecture and mechanical forces to efficiently invade the intestine. This approach will enable molecular and mechanistic interrogation of human-restricted enteric pathogens.

INTRODUCTION

The human intestine is lined by a monolayer of epithelium, which acts as a gatekeeper against infectious microorganisms. During the past decades, much has been learned regarding the molecular machineries leveraged or employed by pathogens to invade this epithelial barrier (Ferrari and Sansonetti, 2016). However, how pathogens interact with their host at the tissue microenvironment remains elusive. Although growing evidence indicates that physical forces can alter the pathogenicity of bacteria, as illustrated by the pioneering work revealing that the shear stress encountered in the urinary tract enhanced type 1 fimbriae-mediated *Escherichia coli* bacterial adhesion (Thomas et al., 2002), the role of the mechanical forces on host-pathogen interactions remains hard to assess.

Shigella flexneri is an enteroinvasive bacterium inducing bacillary dysentery restricted to the human colon. At the molecular and cellular levels, *Shigella* invasion depends on a type III secretion system (T3SS) that translocates about 30 effector proteins into the cytosol of its target cell (Parsot, 2009). Inside its host cell, the bacteria lyses its vacuolar membrane, replicates, spreads into adjacent cells, and reprograms cells to express pro-inflammatory mediators (Ashida et al., 2015), resulting in the destruction of the epithelium. Moreover *Shigella* does not express flagellum or adhesin, although IcsA was shown in some conditions to confer to the bacterium adhesive functions (Brotcke Zumsteg et al., 2014). Although lack of these apparatuses could be advantageous to escape the immune response, it might also be a drawback with respect to adherence and invasion capacities. As is well known, the intestinal epithelium continuously imposes two main physical forces on a colonizing pathogen, i.e., shear stress induced by the intestinal flow, and tensile forces induced by stretching of the underlying muscle layer and resulting in the peristalsis, which may overcome the infectivity of pathogens (Gayer and Basson, 2009; Womack et al., 1987).

While the intracellular life of *Shigella* has been extensively studied in single-cell models, few studies have provided a mechanistic view of the pathogen-colonic tissue interactions (Arena et al., 2015), primarily due to the difficulty of real-time imaging of transient events *in vivo*, using human relevant small-animal models. Moreover, clinical data clearly show that the ingestion of only few hundreds of bacteria is sufficient to trigger diarrheal symptoms in humans (DuPont et al., 1989; Kotloff et al., 1995). However, *Shigella* is notoriously inefficient in infecting polarized epithelial monolayers from the apical surface in the standard, static *in vitro* models (i.e., Transwell system) using either human colon cell line (Mounier et al., 1992) or the recently developed enteroids from human colorectal biopsies (Koestler et al., 2019; Ranganathan et al., 2019). This gap between *in vivo* and *in vitro* results might reflect the oversimplification of the intestinal

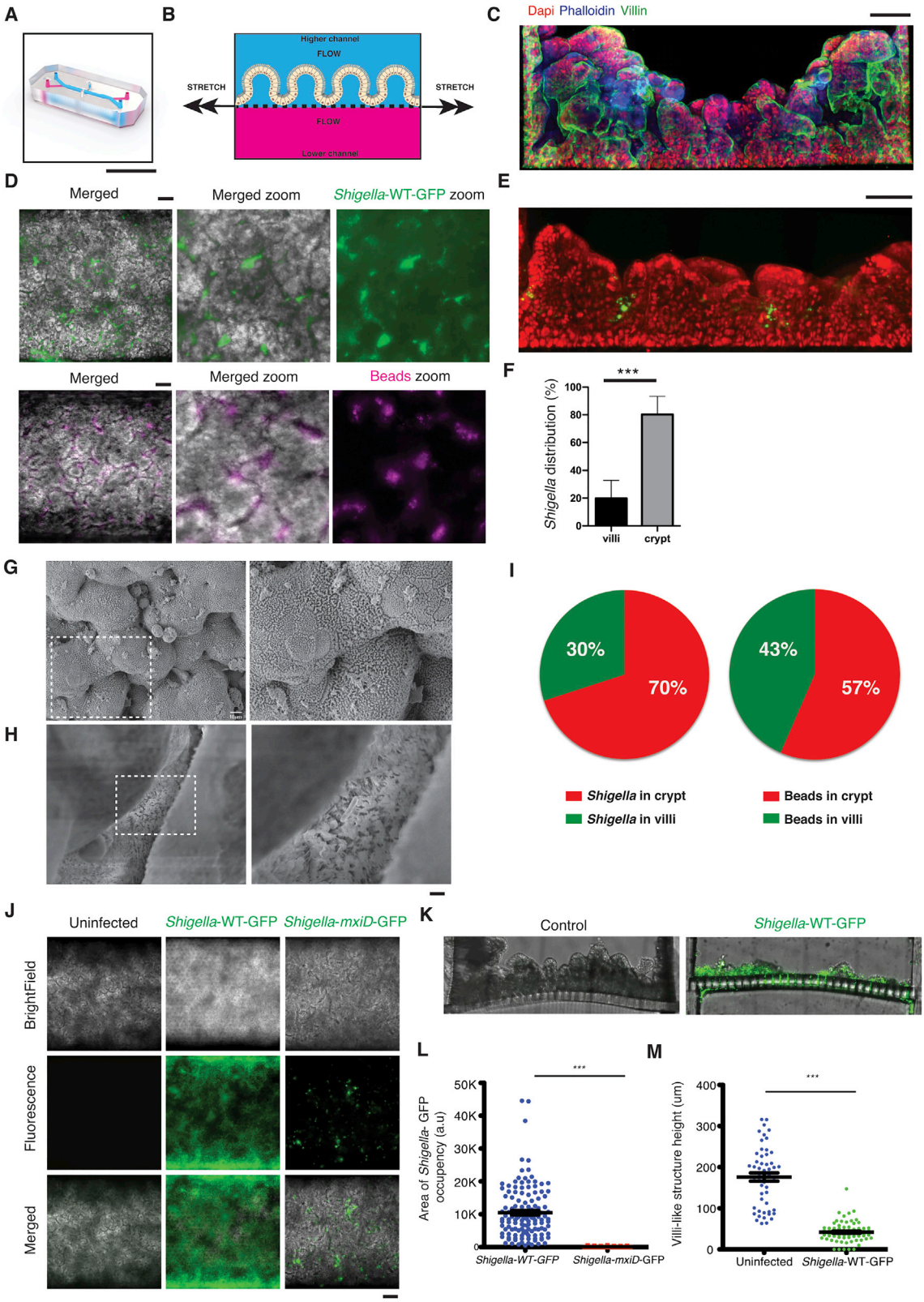


Figure 1. *Shigella* Infection in Intestine-Chip

(A) A photograph of the Intestine-Chip. Scale bar represents 1 cm.

(B) Scheme of a frontal plane of an Intestine-Chip central channel. Upper channel is blue and lower channel is pink. Lateral arrows represent lateral stretching by the side chambers.

(legend continued on next page)

epithelial microenvironment in the conventional *in vitro* models. Recently, advances in Organ-on-Chip technology and microengineering have demonstrated the increased capabilities to recreate important aspects of the intestinal barrier physiology *in vitro* (Kim and Ingber, 2013; Kim et al., 2016). In this study, we employ this approach and use the Intestine-Chip to study *S. flexneri* infection and demonstrate that *in vivo*-like mechanical forces increase the capability of this bacterium to invade the human colonic epithelium.

RESULTS

We set up an Organ-on-Chip approach that recreates a human 3D colonic epithelium and its microenvironmental physical cues (luminal fluidic flow and peristaltic motions) as previously published (Kim et al., 2016). Briefly, we used the Intestine-Chip system made of an elastomeric polymer polydimethylsiloxane (PDMS) (Figure 1A), which consists of (1) a central channel separated vertically by a stretchable porous membrane and (2) two hollow vacuum channels framing laterally the central channel (Figure 1B). The application of cyclic vacuum within these channels induces strain and stretching of the porous membrane that recreate peristaltic-like motions (Kim et al., 2016; Kim and Ingber, 2013). To support the culture of human colonic epithelial cells (Caco-2 cell line, clone TC7), the separating membrane was coated with extracellular matrix (ECM). To recapitulate the physiological microenvironment of the intestine, the seeded cells were exposed for 5 to 6 days to continuous flow (30 μL/h, about 0.0009 dyne cm^{-2}) to recreate the sheer stress on the apical side of the epithelium and to cyclic mechanical strain (10% at a frequency of 0.15 Hz) to reproduce the peristaltic motions (Chaturvedi et al., 2008; Gayer and Basson, 2009; Kim et al., 2012; Womack et al., 1987). Cells grown under these conditions self-organized into villi-like structures interspaced by crypt-like invaginations (Figures 1C and S1A) as previously shown (Kim and Ingber, 2013). In a first step, we confirmed that the seeded Caco-2 cells were polarized and exhibited known differentiation markers (E-cadherin, villin, and FABP1-KRT20) (Figures 1C, S1B, and S1C). Scanning electron microscopy (SEM) imaging also showed microvilli on the apical surface, a typical structural marker of differentiated and polarized enterocytes (Figure 1G). The multicellular villi/crypt-like tissue architecture was also clearly visible by SEM. Finally, we confirmed the impermeability of the epithelial barrier by measuring the diffusion of Dextran-FITC through the monolayer (Figure S1D). Therefore, Intestine-Chip cultures developed a differentiated and mature 3D enterocyte cytoarchitecture.

In order to address whether *Shigella flexneri* could infect the human colon epithelium in the chip, we introduced a wild-type strain expressing GFP (*Shigella*-WT-GFP) in the intestinal lumen of an Intestine-Chip; images were acquired 30, 60, and 120 min post-inoculation (Figures 1D, 1E, and S2A). While individual *S. flexneri* were hardly visible at 30 min using epifluorescence microscopy, we observed a preferential enrichment of *Shigella*-WT-GFP within the interstitial spaces between villi-like structures at 1 and 2 h following inoculation (Figures 1D, 1E, and S2A). By analyzing fluorescent microscopy images for the distribution of *Shigella* associated with the epithelium surface at 1-h post-challenge, we found that about 80% of bacteria were located within interstitial spaces (Figures 1E and 1F). We also confirmed these results at an ultrastructural level in which a majority of *Shigella* (about 70%) were also localized within crypt-like structures (Figures 1H and 1I). To test whether this specific localization or homing is reflecting operation of an active mechanism or not, we investigated the distribution of fluorescent polystyrene beads at the epithelial surface. We observed that a majority of beads were similarly abundant within interstitial spaces, albeit to a lesser extent than the bacteria (Figures 1D and 1I). Taken together, these results suggest that *Shigella* is most likely passively trapped within these intestinal tissue-specific spaces. This precise localization is reminiscent of *in vivo* observations indicating the association of *S. flexneri* with the crypts of colonocytes early in the infection process (Arena et al., 2015). However, we found that these sites were permissive for bacterial colonization, only under physiological luminal flow rates, since a 10-fold increase in flow abrogated the bacterial enrichment (Figures S1E

(C) Stitched images showing intestinal protrusions from a frontal cross-section. Slices were acquired on a swept confocal microscope and Z projected. Cells were fixed, permeabilized, and stained for actin (phalloidin-Alexa647, blue) with anti-villin-1 (green) and nuclei with DAPI (red). Scale bar represents 100 μm.
(D) Representative view of a *Shigella*-WT-GFP-infected chip after 60 min of bacterial exposure (top) or polystyrene beads coated with AlexaFluor-350 (bottom). Merge (left), zoom from merge (middle), and zoom of GFP fluorescence or AlexaFluor-350 (right) images are shown. Scale bar represents 100 μm.
(E) Stitched images showing a cross-section of an Intestine-Chip infected by *Shigella*-WT-GFP (green) for 1 h. Nuclei were stained with Dapi (red). Scale bar represents 100 μm.
(F) Quantification of *Shigella*-WT-GFP distribution within crypt or villi structures from cross-section images of epithelium grown in Intestine-Chip (n = 8). Unpaired Student's t test, ***$p < 0.0001$.
(G) Representative SEM images of epithelium grown in an Intestine-Chip. A magnification of the white dotted area (left) is shown on the right. Scale bar represents 1.3 μm.
(H) Representative SEM images of epithelium grown in a Intestine-Chip and challenged with *Shigella*-WT-GFP-infected chip for 1 h. A magnification of the white dotted area (left) is shown on the right. Scale bar represents 1.3 μm.
(I) Quantification of *Shigella*-WT (left, n = 40) and polystyrene bead (right, N = 23) distribution within crypt or villi from SEM images. Intestine-Chips were infected for 1 h.
(J) Representative images of Intestine-Chip uninfected (left), infected by *Shigella*-WT-GFP (middle), and infected by *Shigella-mxiD*-GFP. Brightfield (top), GFP fluorescent (middle), and merged (bottom) images. Infection was performed overnight. Scale bar represents 100 μm.
(K) Frontal cross-sections of uninfected control (left) and *Shigella*-WT-GFP (green)-infected chips (right). Brightfield (top), GFP fluorescent (middle), and merged (bottom) images. Infection was performed overnight. Scale bar represents 100 μm.
(L) Quantification of *Shigella*-WT-GFP and *Shigella-mxiD*-GFP surface occupancy. Area of all detected individual GFP spots from 15 fields of view from a representative chip is shown. Mean ± SD, n = 135 for *Shigella*-WT-GFP, n = 633 for *Shigella-mxiD*-GFP. Unpaired Student's t test, ***$p < 0.0001$.
(M) Quantification of epithelial villi-like structures height (mean ± SD, uninfected n = 53 from 4 different slices, and *Shigella*-WT-GFP n = 76 from 5 different slices). Unpaired Student's t test, ***$p < 0.0001$.

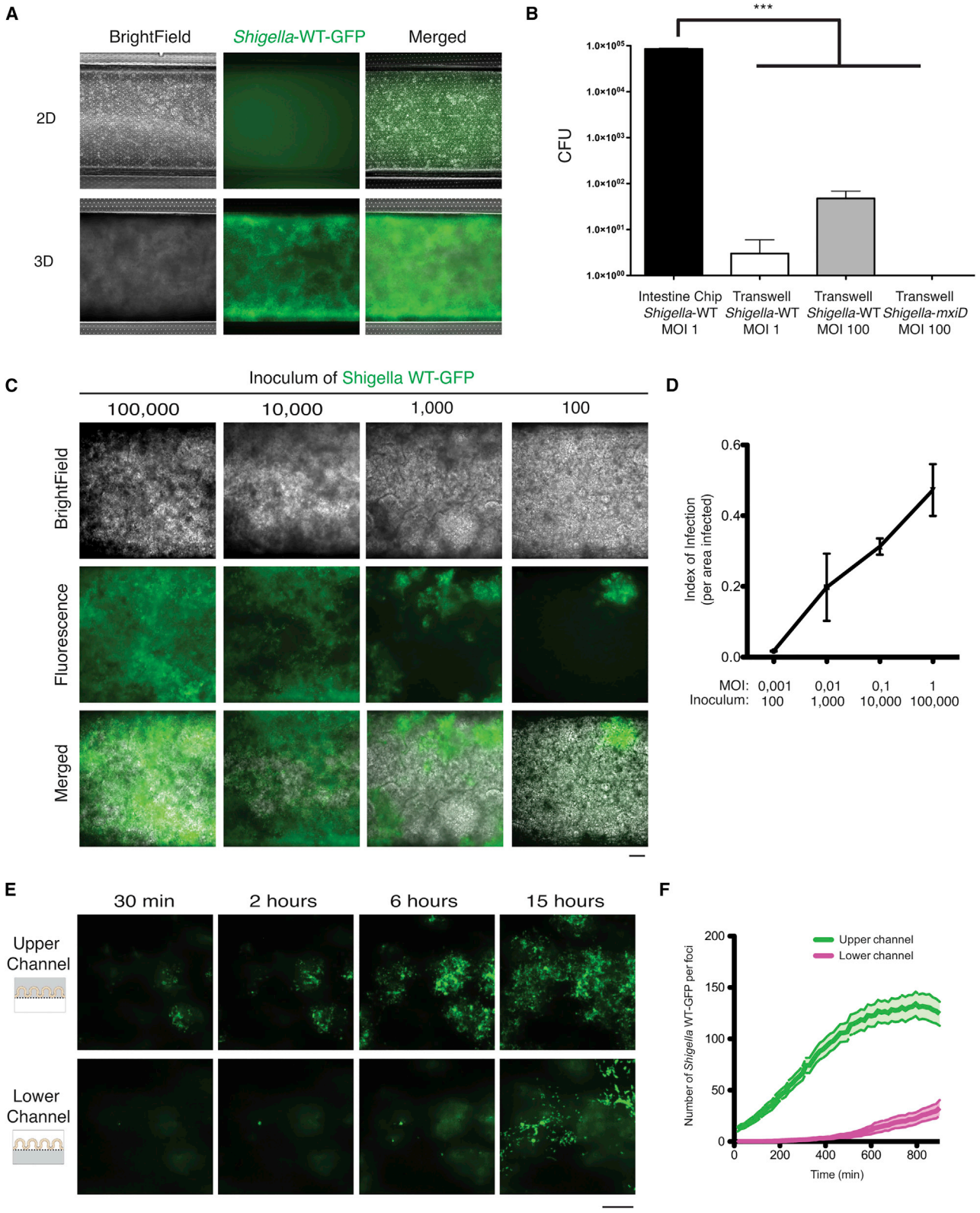


Figure 2. Effect of Epithelial 3D Architecture on *Shigella* Infection in Intestine-Chip

(A) Top view of chips infected overnight with *Shigella*-WT-GFP (green). Before infection, Caco-2 cells were cultured for 2 days (flat -2D) epithelium (top) or for 6 days (3D epithelium) (bottom). Brightfield (left), GFP fluorescent (middle), and merge (right) images are shown. Scale bar represents 100 μm.

(legend continued on next page)

and S1F). Finally, we tested whether *Shigella* could actually invade the epithelium. To do so, we introduced *Shigella*-WT-GFP in the chip lumen using a multiplicity of infection (MOI) of 1 at 37°C under physiological flow and peristaltic motion. Two hours later, non-adhering bacteria were washed away and the infection was left to continue overnight. We observed a strong propagation of *Shigella*-WT-GFP within the entire central channel of the chip (Figures 1J–1L). Furthermore, bacterial invasion was associated with significant changes in epithelium morphology, including loss of the villi-like 3D structures. Specifically, cross-section imaging of the infected chip showed a striking destruction of the epithelial monolayer (Figure 1K) and a significant decrease of approximately 75% in the villi-like height (Figure 1M). We also were able to clearly detect *Shigella* inside the remaining cells, as confirmed by intra- and extracellular bacterial immunostaining (Figure S2B), as well as in the pores of the PDMS membrane that supports the epithelial cell culture (Figure 1K). These results clearly indicate a directional and polarized infection from the apical to the bottom of the epithelial invaginations, in agreement with *in vivo* data showing spreading of *Shigella* across the whole colonic mucosal depth over time. However, it should be noted that disrupting cellular junctions by chelating calcium (EGTA), thereby allowing access to the basolateral side of the monolayer, increased the invasion of *S. flexneri* by 18-fold (Figure S4D). Importantly, we also observed that the non-invasive *Shigella-mxiD*-GFP mutant strain that does not secrete *Shigella* effectors, although recruited in the epithelial invaginations, led neither to foci formation nor to destruction of the epithelium morphology, as compared to the *Shigella*-WT-GFP (Figures 1J and 1L). Thus, the invasion of the Intestine-Chip with *Shigella*-WT-GFP is T3SS-dependent. Moreover, although infection with an *icsA* mutant strain of *Shigella*, a motility-deficient mutant (Bernardini et al., 1989) that is lacking cell-to-cell spreading capacity, led to cell infection, it did not result in the formation of large foci of epithelial destruction (Figure S3C). Altogether, these results show that the Intestine-Chip microenvironment recapitulates the main characteristics of *S. flexneri* invasion of the enterocyte monolayer *in vivo*.

To assess the importance of the colon 3D environment, we performed *S. flexneri* infection on Caco-2 cells cultured *in vitro* on conventional Transwell for 3 weeks, using an MOI of 1 or 100. As previously observed, WT *S. flexneri* failed to efficiently infect the polarized Caco-2 cell-based monolayer on Transwell, introduced from the apical side of the culture (Figure 2B) (Mounier et al., 1992). To quantify the efficiency of *S. flexneri* invasion, we introduced WT bacteria apically to monolayers matured either on Transwell or on Intestine-Chip, and after 2 h of invasion, extracellular bacteria were eliminated by gentamycin treatment for 1 h before plating and counting the colonies (CFU; Figure 2B). Strikingly, maturation in the Intestine-Chip enhanced the *Shigella* invasion by 10,000-fold, as compared to the Transwell (Figure 2B). We also infected flat epithelium grown for only 2 days in the Intestine-Chip under flow and peristalsis, a maturation stage where no 3D villi-like formations are visible yet; we did not observe any infection foci (Figure 2A). Altogether, these results reveal that a 3D-like architecture is essential for efficient *S. flexneri* invasion of the epithelium at the early stages of infection.

In a second step, we wanted to further explore the sensitivity of the Intestine-Chip system for *Shigella* infection. Thus, we exposed the epithelium to various inoculation densities, using a range from 100,000 down to only 100 *Shigella*-WT-GFP bacteria (corresponding to MOI of 1 and MOI of 0.001, respectively), for 2 h, and assessed its invasion using a protective assay strategy. After washing and overnight incubation with gentamicin, we observed that WT *Shigella* was highly efficient in invading the colonic epithelium (Figures 2C and 2D). Strikingly, even a few hundreds of bacteria were sufficient to generate infection foci (Figures 2C and 2D) in the Intestine-Chip, an efficiency close to the data reported from the clinic (DuPont et al., 1989). This suggests that the Intestine-Chip can recapitulate essential cues of the human colonic microenvironment required for *Shigella* infection.

Next, we performed live imaging in order to gain insights into the infection dynamics. We analyzed the expansion of bacterial foci into the epithelial barrier, leading to the consecutive invasion of bacteria into the lower channel (Figures 2E and 2F). With this experiment, we demonstrated that foci could indeed be initiated from a single bacterium alone and revealed that epithelial barrier can be crossed by *Shigella* around 5 h post-initiation of the infection. By measuring the number of bacteria over time, we estimated that the epithelium was disrupted when these foci reached a density of approximately 70 bacteria (Figure 2F). Importantly, the bacterial appearance into the basal channel was not linked to a major leakage since 70 kDa Dextran-FITC was not recovered in the basal channel of infected chips (Figure S1D). Furthermore, we observed that polystyrene beads (1 μm in diameter) also failed to cross through the pores of the supporting membrane during infection (Figure S4A). Finally, we observed that the crossing of *S. flexneri* through the epithelial barrier did not result from massive cells apoptosis (Figure S4B). These data indicate that *Shigella* propagation and crossing

(B) Quantification of epithelium infection by *Shigella*. Epithelium were grown in Intestine-Chip or Transwell and infected apically for 2 h using MOIs of 1 and 100. As a control, infection of *Shigella*-mxiD was performed at an MOI of 100. Then, extracellular bacteria were removed by washes and 1-h gentamicin treatment. *Shigella* were collected by epithelium lysis and CFUs were determined by plating dilution series of lysates. Data represent mean of n = 2 for Intestine-Chip and n = 3 for each condition of Transwell. Errors bars represent standard error of the mean and statistics were performed using a one-way ANOVA with Bonferroni's multiple comparison test, ***$p < 0.0001$.

(C) Representative images of an Intestine-Chip matured for 6 days under intestinal physiological conditions and infected for 2 h with *Shigella*-WT-GFP inoculum of 100,000 CFU (left), 10,000 CFU (middle left), 1,000 CFU (middle right), or 100 CFU (right) before replacement of cell culture media supplemented with gentamicin overnight. Brightfield (top), GFP fluorescent (middle), and merge (bottom) images are shown. Scale bar represents 100 μm.

(D) Quantification of *Shigella*-WT-GFP infection area by immunofluorescence. Index represents the total surface of detected foci per condition divided by the sum of total surface of all conditions. Results are cumulative from 2 separate experiments.

(E) Representative images of time-lapse live imaging of Intestine-Chip infected by *Shigella*-WT-GFP. Events detected in the upper channel (top) and in the lower channel (bottom) are shown after 30 min (left), 2 h (middle left), 6 h (middle right), and 15 h (right). Scale bar represents 100 μm.

(F) Quantification of the number of bacteria detected per focus over time in the upper channel (green) and lower channel (pink), n = 16 foci.

through the monolayer is a direct intracellular mechanism and not a paracellular and passive one.

Then, we addressed whether recapitulation of the physiological mechanical forces (shear stress and peristaltic motions) in the 3D- and 2D-matured intestinal epithelial layer had an impact on the *Shigella* infection process. To better understand their roles in virulence, we investigated each of these parameters at different key steps of the infection: bacterial adhesion, invasion, and propagation (Figures 3 and 4). First, we analyzed the adhesion step by apically exposing Intestine-Chips to *Shigella* for 1 h to avoid most of their uptake (Figures 3A–3C). We did not observe any significant difference in CFU between the different conditions tested (Figure 3B). However, bacteria at this stage of infection remain extracellular and gentamycin protection could not be performed to distinguish bacteria that failed to be washed away. Thus, CFU values might reflect the presence of a mixture of adherent and non-adherent bacteria. To circumvent this technical limitation, we also analyzed images from Intestine-Chip sections we could wash more extensively. In addition, we took advantage of a modified *S. flexneri* strain encoding a transcription-based secretion activity reporter (TSAR) that expresses GFP only upon T3SS induction, which should occur when *Shigella* gets in contact with the host cell (Campbell-Valois et al., 2014). By counting the number of bacteria that were T3SS activated (GFP positive), we observed a drastic difference between 3D and 2D monolayers, regardless of other physical stimuli (Figures 3A and 3C). This result demonstrates that *S. flexneri* adhesion to the cell is dependent on the tissue microenvironment, in particular on the crypt-like structures. In addition, the putative *S. flexneri* adhesin, IcsA, had no impact on the number of adhering bacteria (Figure S3B). Then, we analyzed the role of the microenvironment and mechanical forces in the invasion step: the uptake of *Shigella* into epithelial cells. To do so, we apically challenged Intestine-Chips with bacteria for 2 h, and washed and eliminated remaining extracellular bacteria by gentamycin treatment for another hour before plating and counting CFUs (Figures 3D and 3E). Strikingly, we observed a strong invasion only in 3D epithelium that was mechanically stimulated by stretching tensile forces (Figures 3D and 3E). This indicates that apical invasion of the epithelium by *Shigella* strongly depends on peristaltic motions. Finally, we analyzed the impact of each of these conditions in the capacity of *S. flexneri* propagation in Intestine-Chips protected by gentamycin for 13 h after an initial infection challenge for 2 h (Figure 4). As expected, we observed an important increase of CFUs (around 10^6 CFUs, about 15-fold increase) as compared to the invasion time point, although only in infected 3D cultured Intestine-Chips. However, we noticed that the absence of any mechanical stimulation (such as flow and stretch) limited the bacterial propagation by 60% (Figures 4A and 4B). This suggests that mechanical forces exerted by both flow and stretching enhance the bacterial propagation in the 3D monolayers. To better fine-tune the propagation step, we analyzed the area of the bacterial invasion by performing an image analysis of 3D-matured Intestine-Chips infected as previously, although at a low bacterial inoculum (MOI 0.05) in order to be able to precisely quantify the number of bacterial foci (Figures 4C–4E). In the absence of any applied mechanical stimulation, the total infected area was reduced by about 60% when compared to normal fully actuated conditions (Figures 4C and 4D). The reintroduction of flow alone did not significantly affect infection area when compared to non-mechanically stimulated conditions. In contrast, we observed that the application of stretching forces (peristalsis) significantly increased the efficiency of infection by approximately 50%, as reflected in the number and size of foci (Figures 4C and 4E). Although these results suggest that intestinal flow alone does not significantly increase *Shigella* infection area, they strongly suggest that it facilitates the bacterial multiplication (Figure 4B), and moreover, this was tightly controlled, since exposure to a faster flow rate inhibited the invasion dramatically (Figure S1E) (about 90%).

Overall, our results show that recreation of the architecture and mechanical forces of the intestine strongly impact several stages of *Shigella* infection. First, the bacterial adhesion is favored by the tissue architecture in 3D, enabling a strong T3SS activation once bacteria reach crypt-like areas of the colonic epithelia. Then, bacterial invasion from the apical side of the epithelium is strongly boosted by peristaltic motion, and finally, the propagation is further facilitated upon physiologically relevant sheer stress created by flow.

DISCUSSION

Historically, the Transwell system and polarized Caco-2 epithelial cells have been extensively used for studying *Shigella* infection *in vitro*. While enterocytes are the major cell type of the intestinal epithelium, invasion of cells from the apical side of epithelial monolayer cultured on Transwell has been surprisingly inefficient (Mounier et al., 1992). However, clinical data have been reported showing that only a few hundred to a few thousands of bacteria were sufficient to cause diarrheal symptoms (DuPont et al., 1989). Since *Shigella* invades M cells *in vivo* (Sansonetti et al., 1996), the following dogmatic model has thus been proposed: *Shigella* initially invades the epithelium through M cells from the Peyer's patch and subsequently invades adjacent enterocytes by basolateral spreading. In the present study, we observed that *Shigella* could also invade directly and very efficiently when applied via the lumenal side of the intestinal epithelium composed solely of enterocytes, assuming cells are cultured in 3D *in vivo*-relevant microenvironment. While the 3D maturation of the epithelial layer exposed to mechanical forces is known to induce changes in Caco-2 transcriptome (Kim et al., 2016), $Caco_2$ cell culture on Intestine-Chip does not lead to M cell differentiation, as one of their specific markers, GP2, is not detected on-chip (Kim et al., 2016). Therefore, our results underscore the existence of multiple cellular routes also employed by *Shigella* to successfully invade the intestinal epithelium and indicate that the M cell model is not exclusive. With the current studies, we provide strong evidence on the importance of the previously unappreciated role of the microenvironment, including 3D tissue architecture and mechanical forces, in *S. flexneri* infection. Our data suggest that the organization of the epithelial monolayer in developing 3D crypt-like structures provides a safe niche that is very important in protecting bacteria against luminal flow, thus enabling their adhesion and subsequent activation of the T3SS. Further, our data uncover the contribution of peristalsis, as it greatly enhanced *Shigella* invasion. This result might reflect change in their deposited ECM, affecting the stiffness of the membrane and/or relaxation of the

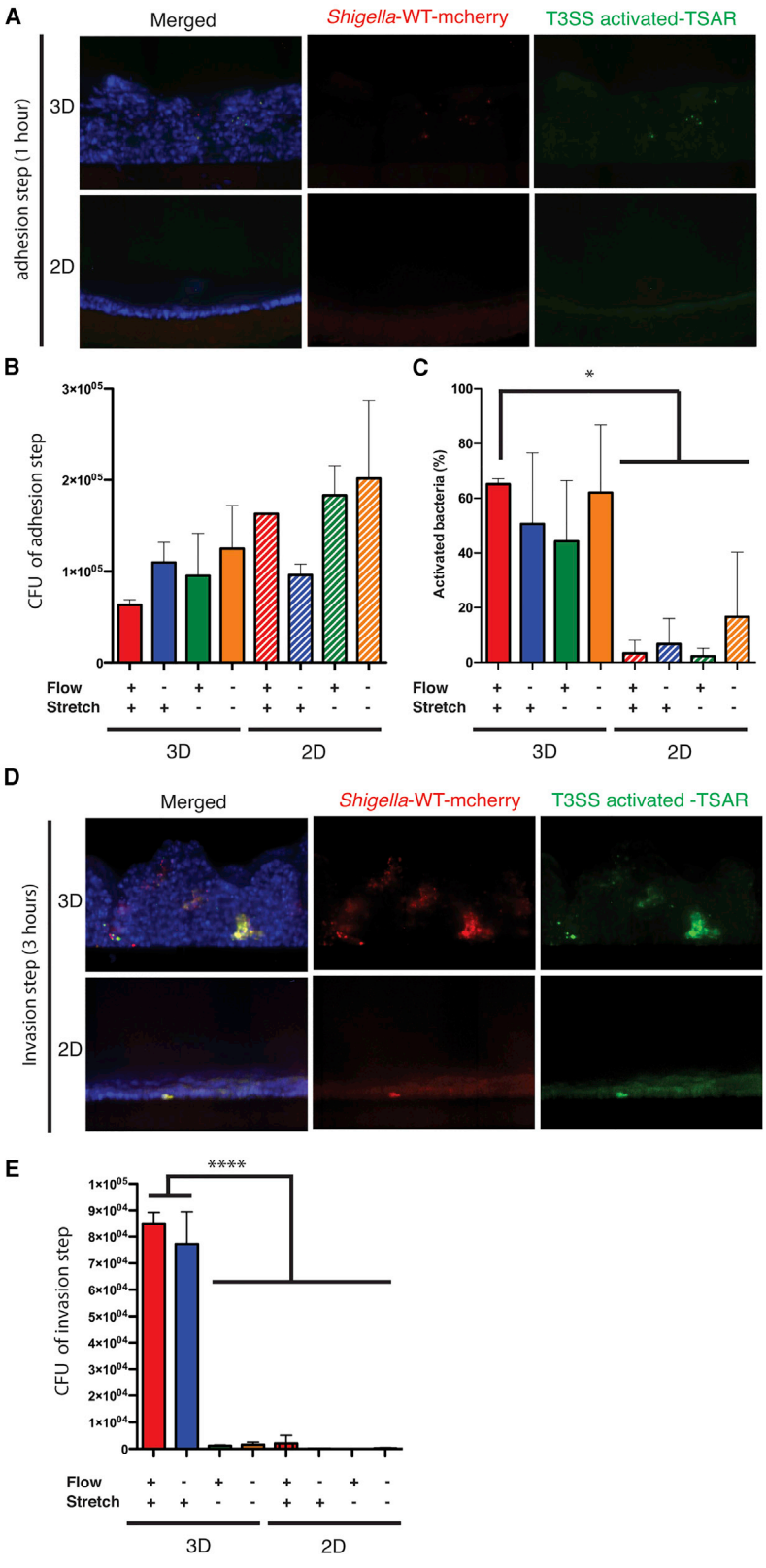


Figure 3. Effect of Mechanical Forces on *Shigella* Infection during Adhesion and Invasion Steps in Intestine-Chip

(A) Stitched images showing cross-sections of epithelium grown in 3D (top) or 2D (bottom) in Intestine-Chip and infected for 1 h (adhesion step) by *Shigella*-WT-mCherry (red) expressing the fluorescent reporter TSAR (green). Nuclei were stained with Dapi (red).

(B) Quantification of *Shigella* adhesion by CFU counting. No significant differences were observed between different conditions using one-way ANOVA with multiple comparisons test.

(C) Quantification of the percentage of the number of activated bacteria detected by TSAR (green) relative to the total number of bacteria (red) after 1 h of infection in epithelium grown in 3D or 2D in Intestine-Chip under application of mechanical forces. Data represent the mean ± SD of 2 chips from 2 independent experiments. Statistics were performed using a one-way ANOVA with multiple comparisons test. *$p < 0.01$.

(D) Stitched images showing cross-sections of epithelium grown in 3D (top) or 2D (bottom) in Intestine-Chip and infected for 3 h (invasion step) by *Shigella*-WT-mCherry (red) expressing the fluorescent reporter TSAR (green). Nuclei were stained with Dapi (red).

(E) Quantification of *Shigella* invasion by CFU counting. Data represent the mean ± SD of 2 chips from 2 independent experiments. Statistics were performed using one-way ANOVA with multiple comparisons test. ****$p < 0.00001$.

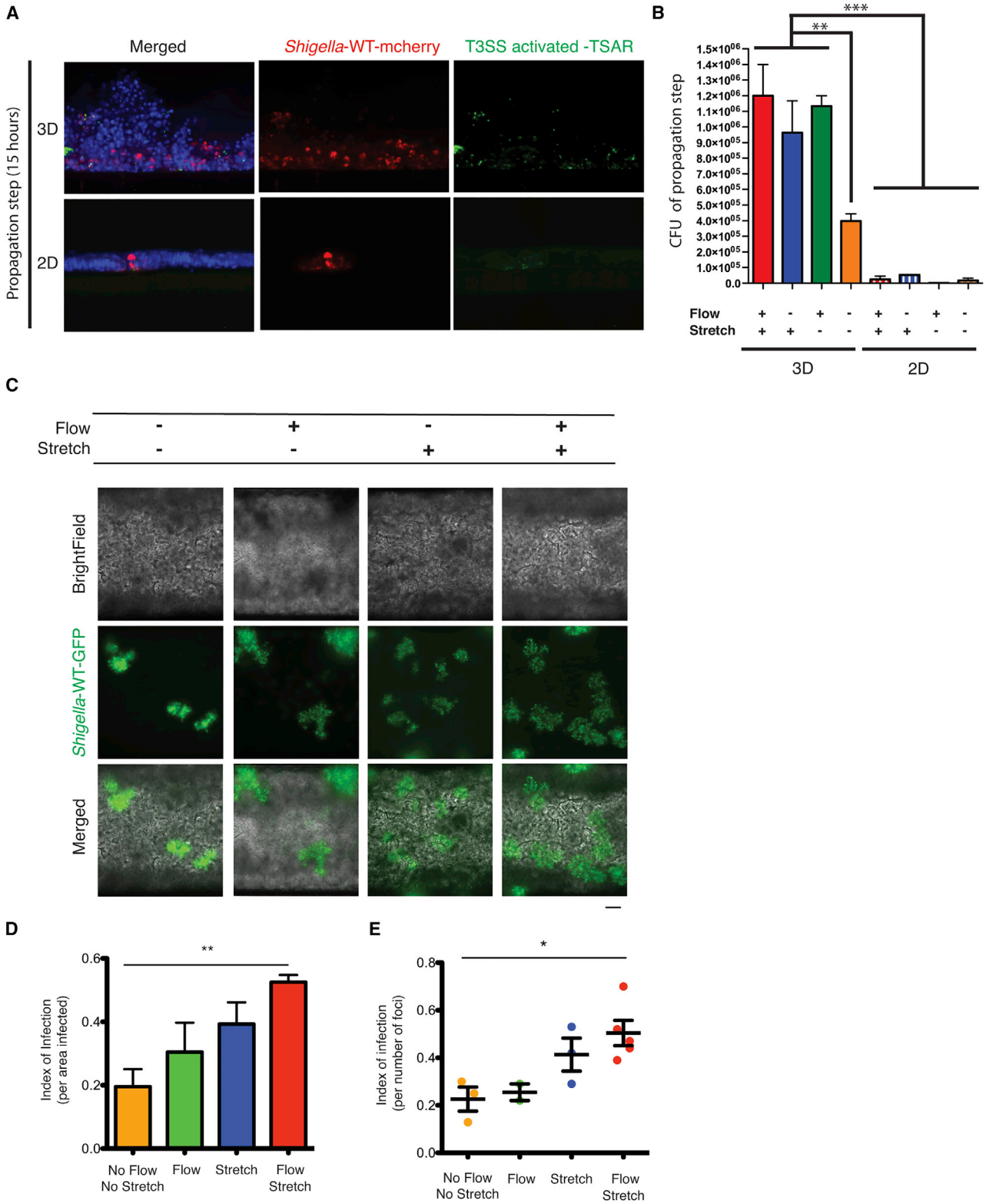


Figure 4. Effect of Mechanical Forces on *Shigella* Infection during the Propagation Step in Intestine-Chip

(A) Stitched images showing cross-sections of epithelium grown in 3D (top) or 2D (bottom) in Intestine-Chip and infected for 15 h (propagation step) by *Shigella*-WT-mCherry (red) expressing the fluorescent reporter TSAR (green). Nuclei were stained with Dapi (red).

(legend continued on next page)

intercellular junctions, by stretching forces, thereby rendering the epithelium more permissive to the invasion process. It will be important in the future to determine the exact mechanism by which stretching forces modulate *Shigella* infection.

Over the years, many models have been developed to study *Shigella* infection. On one hand, small-animal models have been tremendously helpful to understand the pathogenicity *in vivo* (Arena et al., 2015; Sansonetti et al., 1996). On the other hand, standard 2D *in vitro* culture systems contributed to uncovering the molecular mechanisms of infection. Recently, enteroids and stem cell culture emerged as a promising model by providing a more faithful and precise 3D environment *in vitro* (Dutta and Clevers, 2017; Ranganathan et al., 2019; Koestler et al., 2019). While each of these models comes with inherent advantages, all have important limitations in uncovering the effects of physical forces the tissue is exposed to *in vivo*. Since a variety of forces are exerted at the intestinal interface in both physiological and disease states, employing new *in vitro* models for interrogating the role of biophysical forces in host-pathogen interactions is necessary. Here, we show that the technology of bioengineered microphysiological systems, as provided by Organs-on-Chips, carries this potential, together with the associated reduction in use of small animals for experimentation. Organs-on-Chips afford the physiological relevant architecture, mechanical forces, and microenvironment. While the advantages of this technology have been shown in drug safety and efficacy testing (Foster et al., 2019), we show here that this model could also be powerful for investigating infection due to human-restricted pathogens and, even more, to provide new insights in this process in a very controlled manner. Thus, the Intestine-Chip model opens new avenues for biomedical research of host-pathogen interactions in a more physiological environment.

STAR★METHODS

Detailed methods are provided in the online version of this paper and include the following:

- KEY RESOURCES TABLE
- LEAD CONTACT AND MATERIALS AVAILABILITY
- EXPERIMENTAL MODEL AND SUBJECT DETAILS
  - Cell Culture and Bacterial Strains
  - Human Intestine-Chip
- METHOD DETAILS
  - Intestine-Chip Infection
  - Transwell Infection
  - Immunofluorescence
  - Light Microscopy
  - Fluorescent Image Analysis
  - Scanning Electron Microscopy
  - Permeability and Viability Assays
- QUANTIFICATION AND STATISTICAL ANALYSIS
- DATA AND CODE AVAILABILITY

SUPPLEMENTAL INFORMATION

Supplemental Information can be found online at https://doi.org/10.1016/j.chom.2019.08.007.

ACKNOWLEDGMENTS

The authors would like to thank Maryse Moya-Nilges and Jacomine Krijnse Locker from the Unité de Bio-Imagerie Ultra-Structurale of Institut Pasteur. We also thank Héloise Mary from the Biomaterials and Microfluidies core facility and P.H. Commere from the Flow Cytometry Facility of Institut Pasteur. We would also like to thank Jacob P. Fraser from Emulate, Inc. for the initial training on the platform. We also thank P. Brodin, M. Ferrari, and F.X. Campbell-Valois for comments and discussion on the manuscript. A.G. was supported by a Roux fellowship from Institut Pasteur, the PTR22-2016 from the Institut Pasteur, the Institut Carnot Pasteur MS, and ANR-17-CE15-0012-01.

AUTHOR CONTRIBUTIONS

A.G. designed and performed most of the experiments and wrote the manuscript. V.M. performed Transwell and immunofluorescence experiments. S.G. participated in dextran permeability experiments. A.S.-R. participated in SEM experiments. J.K. and K.K. provided Intestine-Chips and advice on their use. S.G., A.S.-R., J.K., and K.K. copyedited the manuscript. B.M. and P.S. participated in the funding of the work and the writing of the manuscript. N.S. led the work, participated in its funding, designed experiments, and wrote the manuscript with A.G.

DECLARATION OF INTERESTS

The authors declare no competing interests.

Received: January 9, 2019
Revised: July 11, 2019
Accepted: August 9, 2019
Published: September 3, 2019

REFERENCES

Allaoui, A., Sansonetti, P.J., and Parsot, C. (1993). MxiD, an outer membrane protein necessary for the secretion of the Shigella flexneri Ipa invasins. Mol. Microbiol. *7*, 59–68.

Arena, E.T., Campbell-Valois, F.X., Tinevez, J.Y., Nigro, G., Sachse, M., Moya-Nilges, M., Nothelfer, K., Marteyn, B., Shorte, S.L., and Sansonetti, P.J. (2015). BioImage analysis of Shigella infection reveals targeting of colonic crypts. Proc. Natl. Acad. Sci. USA *112*, E3282–E3290.

Ashida, H., Mimuro, H., and Sasakawa, C. (2015). Shigella manipulates host immune responses by delivering effector proteins with specific roles. Front. Immunol. *6*, 219.

Bernardini, M.L., Mounier, J., d'Hauteville, H., Coquis-Rondon, M., and Sansonetti, P.J. (1989). Identification of icsA, a plasmid locus of Shigella

(B) Quantification of *Shigella* propagation by CFU counting. Data represent the mean ± SD of 2 chips from 2 independent experiments. Statistics were performed using one-way ANOVA with multiple comparisons test. **$p < 0.001$ and ***$p < 0.0001$.
(C) Representative images of *Shigella*-WT-GFP-infected Intestine-Chip under no flow and no peristalsis (left), flow only (middle left), peristalsis only (middle right), or under both flow and peristalsis (right). Brightfield (top), GFP fluorescent (middle), and merge (bottom) images are shown. Chips were infected overnight with cell culture supplemented with gentamicin 2 h after bacterial addition. Scale bar represents 100 μm.
(D) Quantification of *Shigella*-WT-GFP foci spreading for each condition (no flow/no stretch, flow only, stretch only, and flow and stretch). Results are expressed as an index representing the total surface of detected foci for each condition divided by the sum of all conditions. Mean ± SD, n = 242, 79, 337, and 580, respectively, from 28–62 fields of view; 2–5 independent experiments were performed. ANOVA was used with Bonferroni's post test, **$p < 0.005$.
(E) Quantification of infection index relative to the number of foci. Mean ± SD of 2–5 independent experiments. N = 242, 79, 337, and 580 foci, respectively, from 28−62 fields of view. ANOVA was used with Bonferroni's post test, *$p < 0.05$.

flexneri that governs bacterial intra- and intercellular spread through interaction with F-actin. Proc. Natl. Acad. Sci. USA *86*, 3867–3871.

Brotcke Zumsteg, A., Goosmann, C., Brinkmann, V., Morona, R., and Zychlinsky, A. (2014). IcsA is a Shigella flexneri adhesin regulated by the type III secretion system and required for pathogenesis. Cell Host Microbe *15*, 435–445.

Campbell-Valois, F.X., Schnupf, P., Nigro, G., Sachse, M., Sansonetti, P.J., and Parsot, C. (2014). A fluorescent reporter reveals on/off regulation of the Shigella type III secretion apparatus during entry and cell-to-cell spread. Cell Host Microbe *15*, 177–189.

Campbell-Valois, F.X., Sachse, M., Sansonetti, P.J., and Parsot, C. (2015). Escape of actively secreting Shigella flexneri from ATG8/LC3-positive vacuoles formed during cell-to-cell spread is facilitated by IcsB and VirA. MBio *6*, e02567-14.

Chaturvedi, L.S., Gayer, C.P., Marsh, H.M., and Basson, M.D. (2008). Repetitive deformation activates Src-independent FAK-dependent ERK motogenic signals in human Caco-2 intestinal epithelial cells. Am. J. Physiol. Cell Physiol. *294*, C1350–C1361.

de Chaumont, F., Dallongeville, S., Chenouard, N., Hervé, N., Pop, S., Provoost, T., Meas-Yedid, V., Pankajakshan, P., Lecomte, T., Le Montagner, Y., et al. (2012). Icy: an open bioimage informatics platform for extended reproducible research. Nat. Methods *9*, 690–696.

DuPont, H.L., Levine, M.M., Hornick, R.B., and Formal, S.B. (1989). Inoculum size in shigellosis and implications for expected mode of transmission. J. Infect. Dis. *159*, 1126–1128.

Dutta, D., and Clevers, H. (2017). Organoid culture systems to study host-pathogen interactions. Curr. Opin. Immunol. *48*, 15–22.

Ferrari, M.L., and Sansonetti, P.J. (2016). Cellular invasion by bacterial pathogens. In Encyclopedia of cell biology, R.A. Bradshaw and P.D. Stahl, eds. (Academic Press), pp. 784–793.

Foster, A.J., Chouhan, B., Regan, S.L., Rollison, H., Amberntsson, S., Andersson, L.C., Srivastava, A., Darnell, M., Cairns, J., Lazic, S.E., et al. (2019). Integrated in vitro models for hepatic safety and metabolism: evaluation of a human liver-chip and liver spheroid. Arch. Toxicol. *93*, 1021–1037.

Gayer, C.P., and Basson, M.D. (2009). The effects of mechanical forces on intestinal physiology and pathology. Cell. Signal. *21*, 1237–1244.

Kim, H.J., and Ingber, D.E. (2013). Gut-on-a-chip microenvironment induces human intestinal cells to undergo villus differentiation. Integr. Biol. (Camb.) *5*, 1130–1140.

Kim, H.J., Huh, D., Hamilton, G., and Ingber, D.E. (2012). Human gut-on-a-chip inhabited by microbial flora that experiences intestinal peristalsis-like motions and flow. Lab Chip *12*, 2165–2174.

Kim, H.J., Li, H., Collins, J.J., and Ingber, D.E. (2016). Contributions of microbiome and mechanical deformation to intestinal bacterial overgrowth and inflammation in a human gut-on-a-chip. Proc. Natl. Acad. Sci. USA *113*, E7–E15.

Koestler, B.J., Ward, C.M., Fisher, C.R., Rajan, A., Maresso, A.W., and Payne, S.M. (2019). Human intestinal enteroids as a model system of Shigella pathogenesis. Infect. Immun. *87*.

Kotloff, K.L., Nataro, J.P., Losonsky, G.A., Wasserman, S.S., Hale, T.L., Taylor, D.N., Sadoff, J.C., and Levine, M.M. (1995). A modified Shigella volunteer challenge model in which the inoculum is administered with bicarbonate buffer: clinical experience and implications for Shigella infectivity. Vaccine *13*, 1488–1494.

Lagache, T., Grassart, A., Dallongeville, S., Faklaris, O., Sauvonnet, N., Dufour, A., Danglot, L., and Olivo-Marin, J.C. (2018). Mapping molecular assemblies with fluorescence microscopy and object-based spatial statistics. Nat. Commun. *9*, 698.

Mounier, J., Vasselon, T., Hellio, R., Lesourd, M., and Sansonetti, P.J. (1992). Shigella flexneri enters human colonic Caco-2 epithelial cells through the basolateral pole. Infect. Immun. *60*, 237–248.

Parsot, C. (2009). Shigella type III secretion effectors: how, where, when, for what purposes? Curr. Opin. Microbiol. *12*, 110–116.

Ranganathan, S., Doucet, M., Grassel, C.L., Delaine-Elias, B., Zachos, N.C., and Barry, E.M. (2019). Evaluating Shigella flexneri pathogenesis in the human enteroid model. Infect. Immun. *87*.

Sansonetti, P.J., Kopecko, D.J., and Formal, S.B. (1982). Involvement of a plasmid in the invasive ability of Shigella flexneri. Infect. Immun. *35*, 852–860.

Sansonetti, P.J., Arondel, J., Cantey, J.R., Prévost, M.C., and Huerre, M. (1996). Infection of rabbit Peyer's patches by Shigella flexneri: effect of adhesive or invasive bacterial phenotypes on follicle-associated epithelium. Infect. Immun. *64*, 2752–2764.

Schindelin, J., Arganda-Carreras, I., Frise, E., Kaynig, V., Longair, M., Pietzsch, T., Preibisch, S., Rueden, C., Saalfeld, S., Schmid, B., et al. (2012). Fiji: an open-source platform for biological-image analysis. Nat. Methods *9*, 676–682.

Thomas, W.E., Trintchina, E., Forero, M., Vogel, V., and Sokurenko, E.V. (2002). Bacterial adhesion to target cells enhanced by shear force. Cell *109*, 913–923.

Womack, W.A., Barrowman, J.A., Graham, W.H., Benoit, J.N., Kvietys, P.R., and Granger, D.N. (1987). Quantitative assessment of villous motility. Am. J. Physiol. *252*, G250–G256.

STAR★METHODS

KEY RESOURCES TABLE

REAGENT or RESOURCE	SOURCE	IDENTIFIER
Antibodies		
Villin 1	Abcam	Ab739; RRID: AB_305907
FABP1	Sigma-Aldrich	hpa028275; RRID: AB_10600909
Krt20	Dako	M7019; RRID: AB_2133718
ZO-1	Invitrogen	617300; RRID: AB_138452
LPS	Lab in house collection	N/A
Bacterial and Virus Strains		
Shigella flexneri 5a (M90T) WT	Sansonetti et al., 1982	N/A
Shigella flexneri 5a (M90T) *mxiD* mutant	Allaoui et al., 1993	N/A
Shigella flexneri 5a (M90T) *icsA* mutant	Bernardini et al., 1989	N/A
Shigella flexneri 5a (M90T) TSAR	Campbell-Valois et al., 2014	N/A
Chemicals, Peptides, and Recombinant Proteins		
DAPI	Life technologies	D1306; RRID: AB_2629482
Congo Red	Serva	27215.01
Draq7	Abcam	Ab109202
FITC-Dextran 70kd	Thermofisher scientific	D1823
WGA A555	Life technologies	W32464
Alexa Fluor 350 Phalloidin	Life technologies	A22281
Alexa Fluor 657 Phalloidin	Life technologies	A22287
ER-1	Emulate	ER-1
ER-2	Emulate	ER-2
Rat tail Collagen type 1	gibco	A1048301
Matrigel	corning	356234
Critical Commercial Assays		
Intestine-Chip	Emulate	Intestine-Chip
Experimental Models: Cell Lines		
Caco-2	ATCC	clone TC7
Software and Algorithms		
Fiji image software	Schindelin et al., 2012	https://fiji.sc/
ICY	de Chaumont et al., 2012	http://icy.bioimageanalysis.org
Prism 7	GraphPad	http://graphpad.com

LEAD CONTACT AND MATERIALS AVAILABILITY

Further information and requests for resources and reagents should be directed to and will be fulfilled by the Lead Contact, Nathalie Sauvonnet (nathalie.sauvonnet@pasteur.fr).

This study did not generate new unique material.

EXPERIMENTAL MODEL AND SUBJECT DETAILS

Cell Culture and Bacterial Strains

Caco-2 cells (clone TC-7) were obtained from ATCC. Cells were grown in Dulbecco's Modified Eagle Medium (DMEM, Gibco) supplemented with 20 % FBS (fetal bovine serum, Biowest) and non-essential amino acid (Gibco) in 10% CO_2 at 37°C.

The wild type derivative *Shigella flexneri* 5a (M90T) (Sansonetti et al., 1982), the *mxiD* mutant derivative of the wild type strain (Allaoui et al., 1993) and the *icsA* mutant derivative of the wild type strain (Bernardini et al., 1989) were used. All these strains harbor the pFPV25.1 plasmid encoding GFPmut3. TSAR plasmid was described previously (Campbell-Valois et al., 2014, 2015). Bacteria were grown at 37°C on trypticase soy (TCS; Becton Dickinson) agar plates containing 0.01 Congo red (Serva). Individual colonies

were grown at 30°C overnight with ampicillin. From this culture, bacteria were grown at 37°C in TCS to obtain a suspension of 10^{10} CFU/mL.

Human Intestine-Chip

Intestine-Chips made of polydimethylsiloxane (PDMS) and associated instrumentation and software (Human Emulation System) for culturing the chips were obtained from Emulate (Boston, MA).

Chips were activated for ECM coating per manufacturer instructions. Briefly, chips were rinsed in 70% ethanol (Sigma-Aldrich) followed by sterile water (Gibco) and ER-2 solution (Emulate). Then, chips were activated using ER-1 solution (Emulate) and exposed for 20 min under UV light (36W, 365nm). Finally, chips were rinsed with ER-2 solution followed by PBS (Gibco). Then, ECM coating was performed by incubating an ECM solution (100mg/mL of Matrigel (Corning) and 30-μg/mL rat tail Collagen type 1 (Gibco) diluted in DMEM (Gibco)) for 2 hours at 37°C 5% CO_2. Cells were seeded at a concentration of 1.5 millions/mL in the upper channel for 2 hours at 37°C 5% CO_2. After cell attachment, upper channel was gently washed using warm cell culture media supplemented with 100U/mL penicillin and 100μg/mL streptomycin. Cells were maintained statically overnight. Then, chips were connected to the instrument (Emulate) and maintained for the duration of the culture. The following cell culture conditions were applied: 37°C, 5% CO_2, flow at 30μL/hr and 10% of lateral mechanical stretching at a frequency of 0.15 Hz. Cell culture media was equilibrated and refreshed every 48 hours.

METHOD DETAILS

Intestine-Chip Infection

Intestine-Chips were washed overnight at 30μL/hour in regular cell culture media without penicillin and streptomycin in both channels. Then, S. flexneri (neither coated with poly-L-lysine nor expressing exogenous adhesin) were introduced in the top channel from the Pod reservoir. To synchronize the exposure of bacteria over the full surface of the top channel, a fast flow of 400μL/hour for 30 min was performed. The end of this pulse corresponds to time zero. Then, flow and/or stretching conditions were applied for the duration of the experimental condition. To determine the adhesion capacity, infection duration was one hour. At this end of this challenge, chips were washed twice with regular cell culture media using gravity flow. Bacteria were recovered using 0.5 % sodium deoxycholate (Sigma-Aldrich) and diluted lysate series were plated with ampicillin. For immunofluorescence, chips were removed from the instrument at the end of the incubation time and infection was stopped by gently flushing 4% of paraformaldehyde (Electron Microscopy Sciences) diluted in PBS with Ca^{2+} and Mg^{2+} (Gibco) in top and bottom channels.

To determine invasion capacity, infection duration was three hours as follow: after a 2 hours challenge, extracellular bacteria were washed at 400μL/hour for 30 min in cell culture media supplemented with gentamycin at a final concentration of 50μg/mL (ThermoFisher). Then, Intestine-Chip were incubated for an additional 30 min under their mechanical conditions prior bacteria recovery or immunofluorescence processing as described previously. To determine propagation capacity, infection duration was 15 hours as follow: after 2 hours challenge, Intestine-Chip were washed at 400μL/hour for 30 min in cell culture media supplemented with gentamycin at a final concentration of 50μg/mL (ThermoFisher). Then, chips were incubated for 12h30 under their mechanical conditions prior bacteria recovery or immunofluorescence processing as described previously.

For EGTA disruption, Intestine-Chip were briefly rinsed with Calcium free ringer buffer supplemented with 100mM EGTA. Then, infection were performed using this buffer as described for the invasion step assay.

For beads distribution assay, blue fluorescent microspheres (FluoSpheres carboxylate-modified, F8815, Invitrogen), of a diameter of 1μm were used at a concentration of 1 million/mL under the same experimental settings as *Shigella* infection.

Transwell Infection

Caco-2/TC7 cells, $2x10^5$ cells/cm^2 cells were seeded into 12-well or 6-well Transwell inserts (pore size 0.4 μm, Corning) and cultured for 18-21 days at 10% CO_2 at 37°C; fresh media was added triweekly. S. flexneri (neither coated with poly-L-lysine nor expressing exogenous adhesin) were pelleted, washed with PBS and resuspended in infection medium to MOI 1 or 100. Apical and basal chambers were washed twice with warm DMEM-Hepes and bacteria were added to the apical chamber, incubated for 2 hours at 37°C in CO_2 incubator and then apical/basal medium was aspirated and replaced for fresh DMEM-Hepes supplemented with gentamicin 50 μg/mL and incubated for 1 hour at 37°C in CO_2 incubator before recovering bacteria using 0.5 % sodium deoxycholate (Sigma-Aldrich) and plated dilution on ampicillin plates.

Immunofluorescence

Chips were fixed in 4% of paraformaldehyde (Electron Microscopy Sciences) diluted in PBS with Ca^{2+} and Mg^{2+} (Gibco) for 30 min. Top and bottom channels were flushed with PBS after fixation. If the immunostaining was not performed immediately, chips were immersed in cold PBS and stored at 4°C. For transversal sections, chips were cut in 200-μm thick slices using a vibrating blade microtome (VT1000S, Leica). Sections were permeabilized in buffer A (PBS/0.2% Triton X-100/ 0.5% BSA) for 1 hour at room temperature (RT) and incubated with primary antibody diluted in buffer A supplemented with 1% DMSO for 2 hours at RT or overnight at 4°C. Primary antibodies used were:

Antigen	Dilution	Catalogue #	Isotype	Manufacturer
Villin 1	1:200	610358	Mouse IgG_1	BD Biosciences
Villin 1	1 :100	Ab739	Mouse	Abcam
FABP1	1:200	hpa028275	Rabbit	Sigma-Aldrich
Krt20	1:200	M7019	Mouse IgG	Dako
LPS	1:300	in house	Rabbit	in house
ZO-1	1 :100	617300	Rabbit	Invitrogen

Then, chip sections were washed at least 3 times in buffer A for 15 min and stained for 2 hours at RT with secondary antibodies Alexa Fluor A568 or Fluorescein isothiocyanate (FITC) goat anti-mouse or anti-rabbit (Life technologies). Staining with wheat germ agglutinin Alexa Fluor A555 (no. W32464, Life technologies), DAPI (Life technologies) and phalloidin Alexa Fluor A350 or A647 (Life technologies) were performed for 1 hour at RT in Buffer A. Samples were rinsed at least 3 times in PBS and imaged immediately and directly in PBS on coverslips #1.5 (Corning and Matek).

Light Microscopy

Chips under maturation were observed on an automated microscope (Zeiss, Axio observer Z1) equipped with Colibri 2 and camera (Orcaflash 4 v2.0, Hamamatsu). A full scan of the upper channel was performed with a 10x air objective (Zeiss Plan Apochromat 10x 0.45 N.A) in brightfield. Z-series of optical sections was photographed from the porous membrane to the top of the tissue. For infection experiments, a full scan of the upper channel was performed using the 10x objective. This allows capturing all locations of foci of infection of GFP-expressing *S. flexneri*. Exposure time was about 200ms. Regions of interest were also acquired with a 20x air objective (Zeiss Plan Neofluor 20x 0.4 N.A). Sections between 200μm and 300μm-thick were imaged using an Opterra swept confocal microscope (Brucker) mounted on a Zeiss axio observer Z1 and equipped with an EMCCD Evolve 512 Delta camera (Photometrics). Exposure time was about 100-200ms using an EM gain of about 550. Live cell imaging was performed in an environnemental control system set to 37°C and 5 % CO_2. Nemesys low-pressure modules (Cetoni) and pressure controller OB-1 MkIII+ (Elveflow) were used for controlling flow and stretching conditions. Microscopy images were adjusted for brightness, color balance, and/or contrast uniformly across all pixels, as necessary, in image J (v1.46r, National Institutes of Health) or ICY Software (Institut Pasteur).

Fluorescent Image Analysis

To quantify the infection efficiency based on fluorescence images, borders of foci of infection were visually detected and regions of interest (ROI) were hand-drawn using ImageJ. A foci is defined as a surface area infected by *Shigella*. Then, two parameters were measured : the number of detected foci and the area of these detected individual foci. Results are expressed as an index of infection relative either to the number of foci or the surface area of foci. Index of infection is calculated as the total number detected foci for each condition divided by the sum of all.

To quantify the distribution of *Shigella* into crypt or villi like structure from Intestine-Chip sections, we define ROIs corresponding to villi and crypt and used ICY software (http://icy.bioimageanalysis.org) Spot Detector plugin that allow for an automatic bacteria detection. To assess for TSAR activation during the adhesion time-point, the Intestine-Chips were infected with TSAR producing strain for 1 hour. This strain expresses constitutively mCherry and upon T3SS induction also express GFP. After fixation, sections of Intestine-Chips were imaged using an Opterra swept confocal microscope and analysed with ICY software plugins. We used Spot Detector plugin to automatically detect objects corresponding to red and green bacteria (mCherry and GFP) and then we used Colocalization Studio plugin (method: object based and statistical colocalisation, SODA (Lagache et al., 2018), to quantify the number of mCherry bacteria producing GFP, hence TSAR activated.

Scanning Electron Microscopy

Cells were fixed in 2.5 % glutaraldehyde in PHEM buffer (pH 7.0) for 1 hour at RT and washed 3x 5min in distilled H_2O. The top of the upper channel of the chip was open by successive longitudinal 900-μm thick slices using a vibrating blade microtome (VT1000S, Leica). Then, chips were post-fixed with 1% osmium tetroxide in distilled H_2O for 1h and rinsed with distilled H_2O . Cells were then dehydrated through a graded ethanol series (25, 50, 75, 95 and 100 %) followed by critical point drying with a Leica EM CPD 300. Finally dried specimens were sputter coated with a 10 nm gold/palladium conductive layer using a gun ionic evaporator PEC 682. Images were acquired on a JEOL JSM 6700F field emission scanning electron microscope operated at 7kV. Quantification of *Shigella* and beads distribution within crypt and villi structures were manually score in a binary manner (i.e. scored as 1 if at least one bacteria was visually detected in the image or zero if not)

Permeability and Viability Assays

Intestine-Chip were prepared as previously mentioned and maintained under flow (30μL/hour) and stretching conditions (10%, 0,15Hz) for 6 days. An empty Intestine-Chip was used as a control. Each chip was microscopically examined before the assay. FITC-dextran 10 or 70 kDa was briefly introduced to the reservoir of the top channel (10μg/mL) in cell culture media. A brief a pulse

of 400 μL/hour for 30 min was used to synchronize all chips. The end of this pulse corresponds to time zero. After 2 hours to overnight incubation, samples from the top and bottom were collected and fluorescence was measured in a spectrofluorometer (Infinite M200Pro, Tecan, Switzerland) with excitation wavelength of 488 nm and an emission wavelength of 520 nm. Permeability assay were performed from 2 experiments, each of which included 3 different chips.

For live cell imaging experiments, 1μm blue fluorescent microspheres were simultaneously added to cell culture media with Shigella at time 0 of infection. Cell membrane integrity was determined by adding directly the far-red fluorescent dye Draq7 (Ab109202, Abcam) in cell culture media at a final concentration of 3μM for at least 30 min at 37°C.

QUANTIFICATION AND STATISTICAL ANALYSIS

Statistical significance was determines using unpaired Student's *t* test. For multiple comparisons, analysis of variance (ANOVA) was used with Bonferroni's or Dunnett's post test. Statistics were completed using prism 7 (GraphPad, La Jolla, CA). Specific details with regard to statistical tests, as well as, sample sizes (''n'') and replicates can be found in the figure legends. For all analysis, significance was considered $p<0.05$.

DATA AND CODE AVAILABILITY

This study did not generate/analyze datasets and code.